JOURNAL OF AIRCRAFT
Vol. 41, No. 6, November–December 2004

Development of Powered Resonance-Tube Actuators for Aircraft Flow Control Applications

Ganesh Raman* and Andrew Mills†
Illinois Institute of Technology, Chicago, Illinois 60616
and
Valdis Kibens‡
The Boeing Company, St. Louis, Missouri 63166

The present paper addresses both active-flow-control actuator technology development and the demonstration of the effectiveness of actuators that could be easily integrated into practical aircraft applications. The actuator used is an adaptation of the Hartmann oscillator. Demonstration experiments that illustrate the effectiveness of this actuator include cavity tone suppression at transonic speeds and the reduction of jet-impingement tones. The actuator concept is based on a high-speed jet aimed at the mouth of a cylindrical tube closed at the other end. The result is a high-amplitude self-sustaining fluctuating field accompanied by an intense narrowband tone, all in the region between the supply jet and the resonance tube. Using unsteady pressure sensors and flow visualization, we explored the effect of varying actuator parameters such as the spacing between the power jet and the resonance tube, supply pressure, resonance-tube depth, diameter, shape, and lateral spacing. By varying the depth of the tube, the frequency could be varied from about 1.6 kHz to over 10 kHz and amplitudes as high as 156 dB (microphone location dependent) were obtained in the vicinity of actuation. To integrate this concept into practical aircraft applications, two generations of a more complex version of this device known as the powered resonance-tube bank (PRTB) were developed and demonstrated. Results indicate that by using high-frequency excitation at 5-kHz suppression levels in excess of 20 dB were consistently obtained over a range of operating conditions in both cavity and impingement flow situations. Based on our results, we have grounds to believe that a properly designed PRTB has significant advantages over conventional actuators such as acoustic, piezo, and oscillatory microstructures.

Introduction

IN this paper we describe the development of novel powered resonance-tube actuators. The actuators operate over a range of frequencies and produce high amplitudes of pressure fluctuations. Such actuators are attractive alternatives to conventional electromagnetic and piezoelectric actuators. The conventional actuators are fragile and have high power and maintenance requirements. This paper describes our attempts to harness the oscillatory field of the Hartmann oscillator by suitable adaptation and integration. The final result is a high-frequency actuator with no moving parts that can inject high-amplitude fluctuations into a flow that we wish to control. Such actuators could eventually replace steady mass-addition methods with oscillatory addition of fluid at lower mass-flow (bleed) levels. Two examples of applications (cavity and impinging jet) that demonstrate the effectiveness of this type of actuator are also provided.

The role of an actuator is to inject perturbations at a prescribed frequency, amplitude, and mode (spanwise or azimuthal) at locations where the flow is most receptive to these inputs. The actuation then leverages or disrupts the flow to bring about a desired effect. An example of leveraging is the excitation of jet or shear-layer instability modes within their most amplified frequency band that in turn energizes large-scale-coherent structures. The energetic large-scale coherent structures can grow, interact, and engulf surrounding fluid, thus enhancing mixing. Examples of disrupting flow phenomena to bring about a desired change are suppression of cavity or jet-impingement tones. Flow-induced tones are suppressed when the excitation destroys the spanwise coherence or damps out organized structures in the nascent shear layer and prevents the sustenance of the flow-induced resonance. We are particularly interested in the cavity and jet-impingement tone suppression because these situations can cause problems in weapons bays of military aircraft and in short-takeoff-and-vertical-landing aircraft (STOVL). Our objective here is to develop scalable and integrable actuators for use in future military aircraft applications.

In our quest for an ideal actuator, we considered the adaptation of the Hartmann whistle as a high-frequency actuator for use in active flow-control applications. The idea for this adaptation was first suggested by Kibens and Raman in 1998 and was subsequently awarded a U.S. patent. In the following paragraphs we elaborate on our motivation and provide background information on the Hartmann tube before proceeding with the discussion of our adaptation.

Motivation

Our technology development program was motivated by two possible applications.

First, there are weapons-release problems with internal weapons bays of military aircraft. Current military aircraft use passive suppression (spoilers) for reducing the intensity of the acoustic environment in weapons bays. However, these spoilers are ineffective above a Mach number of 1. The goal of the U.S. Air Force is to release weapons above $M = 1$ because this represents a tactical advantage in combat. Our focus therefore is to develop active flow-control (AFC) techniques for cavities that are effective at $M > 1$.

Second, STOVL aircraft problems include lift loss caused by suck-down effects, hot gas reingestion, ground erosion, and sonic fatigue. In addition, high acoustic levels and wall-jet flows on aircraft carriers are of prime concern to ground personnel. There is a need to develop AFC methods to improve the aerodynamic performance of STOVL aircraft in the ground environment. This includes improvement of aircraft stability, lift optimization, and improved

Received 30 October 2002; revision received 26 May 2003; accepted for publication 27 May 2003.

*Associate Professor, Department of Mechanical, Materials and Aerospace Engineering, E1, 10W 32nd Street; Raman@iit.edu. Associate Fellow AIAA.

†Undergraduate Research Participant, Department of Mechanical, Materials and Aerospace Engineering, E1, 10W 32nd Street.

‡Associate Technical Fellow, P.O. Box 516, MS S106-7126; Valdis.Kibens@Boeing.com. Associate Fellow AIAA.

ground-impingement properties (fountain location, suck-down, and pressure distribution on wings).

Background

The resonance-tube phenomenon was first discovered by Hartmann in 1918. He then published several papers in the 1920s and 1930s[1,2] describing the generation of the strong pressure oscillation and intense noise produced by a jet aimed at the open end of a tube closed at the other end. There are two phases of operation of the Hartmann tube. In the first phase the jet penetrates the tube and compresses the air in the tube. The compression produces a shock wave, which is reflected by the end wall of the tube. When the reflected shock wave arrives at the open end of the tube, it interacts with the jet and, under some conditions, pushes it backwards. At this point in time, the second phase of the oscillation begins. In this phase the tube empties itself. In terms of wave dynamics, one can think of an expansion wave moving towards the closed end, being reflected there, and then the reflected expansion wave moving towards the open end of the tube. As this expansion wave approaches the open end of the tube, the low pressure associated with the expansion wave draws the supply jet into the tube, thus perpetuating the oscillatory cycle. The process then repeats itself, thus producing strong pressure oscillations without the use of any moving parts. Nearly 40 years later after Hartmann's discovery, Sprenger[3] found that in long tubes the flow oscillation can produce significant heating of the tube wall. The longer tubes are thus referred to as Hartmann–Sprenger tubes. Subsequently several papers have addressed various aspects of the Hartmann and Hartmann–Sprenger tubes.[4,5] Rakowsky et al.[6] evaluated various powered resonance tubes for rocket engines and weapons ignition systems. The geometries examined included cylindrical, tapered, and stepped tubes. However, their focus was not on the functioning of these devices as actuators but on the maximum temperature that could be generated at the closed end of the tube. The stepped tube was seen to produce the highest temperature [2000°F (1093°C)] at the closed end, followed by the tapered tube [1500°F (816°C)], the cylindrical being the least [1000°F (538°C)]. Other studies on the Hartmann and Hartmann–Sprenger tubes were conducted by Brocher and coworkers.[7–13] High temperatures are obtained in a Hartmann–Sprenger tube only for large tube depths. In the present work the tube depths were all 1.27 cm where thermal effects were not significant.

Note that the resonance-tube phenomenon in itself is not new, but its application as an AFC actuator is unique. Using unsteady pressure sensors and flow visualization, we explored the effect of varying actuator parameters such as the spacing between the power jet and the resonance tube, supply pressure, resonance-tube depth, diameter, shape, and lateral spacing. By varying the depth of the tube between 3/16 and 2 in. (0.476 and 5.08 cm) (depth/diameter, $d/D = 0.75$ to 8), the frequency could be varied from about 1.6 to over 10 kHz. The amplitudes were as high as 156 dB (microphone location dependent) in the vicinity of actuation. The demonstration includes experiments at the Illinois Institute of Technology (IIT), The Boeing Company, and Defense Evaluation and Research Agency (DERA, United Kingdom) on a variety of flow-induced resonance suppression situations.

Search for a High-Frequency Excitation Device

Wiltse and Glezer[14,15] found that exciting a flow in the inertial subrange can significantly alter the energy cascade. Based on Wiltse Glezer's work, Cain suggested in a 1997 private communication that high-frequency excitation would be a very effective method to suppress flow-induced resonance. To verify Cain's idea, Raman et al.[16] conducted several experiments with high-frequency excitation devices. The effort began using piezoelectric actuators to suppress subsonic edgetones (see Fig. 1). Figure 1 shows the edgetone setup using a rectangular jet a $M = 0.07$ impinging on a wedge. Addition of energy at 5130 Hz was seen to suppress all tones (the primary edgetone frequency was 672 Hz). Both tonal and integrated (over the entire frequency spectrum) sound-pressure levels were suppressed. Because piezoactuators are fragile and more suitable for laboratory applications, an effort was made to develop a more practical high-

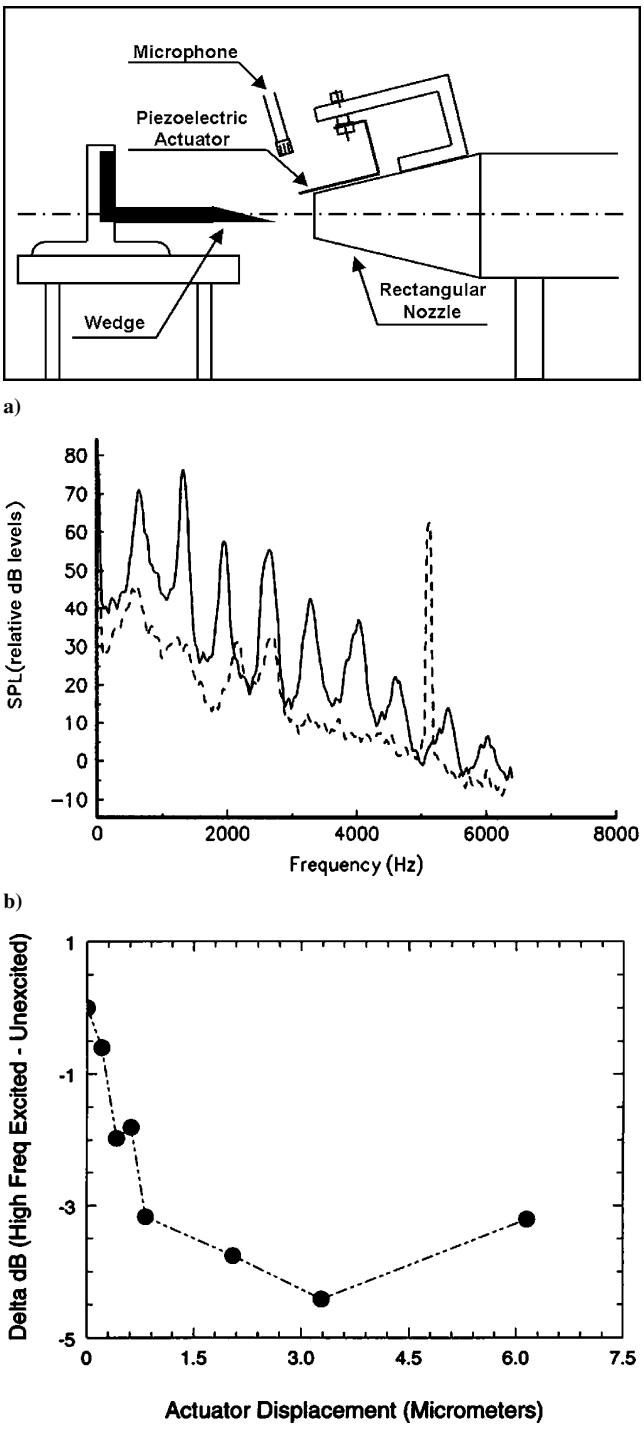

Fig. 1 Edge-tone suppression using high-frequency excitation (via piezoelectric actuators) for the suppression of flow-induced resonance: a) schematic diagram of the setup, b) unsuppressed (——) and suppressed (- - - -) edge-tone spectra, and c) integrated spectral level difference (Δ dB for various actuator displacements).

frequency excitation device. Raman et al.[16] developed and demonstrated powered resonance-tube actuators (see Fig. 2). A powered resonance-tube bank (PRTB) was developed[17] and was subsequently tested by Stanek et al.[18,19] Later Cain et al.[20] also studied the high-frequency excitation phenomenon through simulations of a plane transitional wake. In addition, illustrative flow-visualization images of the functioning of PRT devices is shown in the paper by Kastner and Samimy.[21] In the present paper we study in considerable detail the characteristics of single-and multiple-powered resonance-tube actuators. In particular, we provide a detailed documentation of

Table 1 Summary of powered resonance-tube configurations evaluated

Configuration	Diameter, in. (cm)	Δx, in. (cm)	Δp, psig (NPR)	Frequency range, Hz
Single cylindrical	0.25 (0.635)	0.25–0.625 (0.635–1.588)	30–80 (3.076–6.536)	4,352–6,080
	0.125 (0.3175)	0.25–0.5625 (0.635–1.429)	5–80 (1.346–6.536)	5,120–6,528
	0.0625 (0.1588)	0.0625–0.375 (0.1588–0.953)	5–80 (1.346–6.536)	4,360–7,296
Single stepped	0.25 (0.635)	0.25–0.5625 (0.635–1.429)	3–80 (1.208–6.536)	7,040–11,070
Single tapered	0.25 (0.635)	0.25–0.5625 (0.635–1.429)	1–80 (1.069–6.536)	7,744–11,010
Powered resonance-tube banks	0.25 (7 tubes, 0.635)	0.125–0.6875 (0.3175–1.746)	1.5–33 (1.1–3.3)	4,000–6,400
	0.125 (9 tubes, 0.318)	0.125–0.4375 (0.3175–1.111)	2–50 (1.138–4.460)	4,672–6,016
	0.125 (9 tubes, 0.318)	0.125–0.3125 (0.3175–0.7938)	2–50 (1.138–4.460)	4,800–5,824

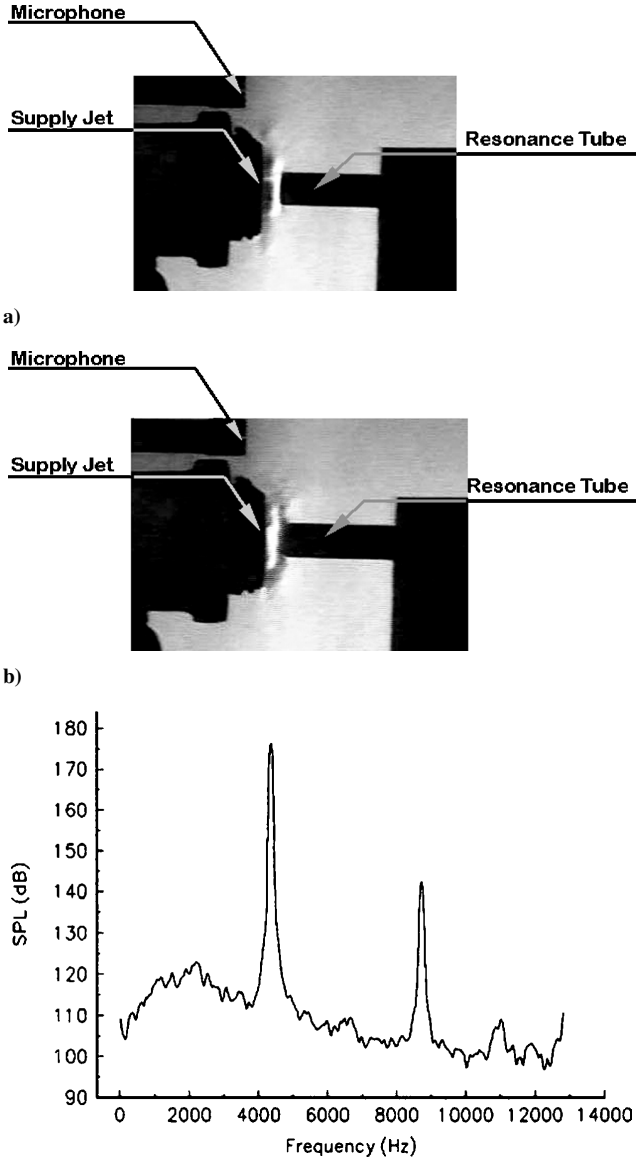

Fig. 2 Experiment demonstrating the performance of the Hartmann whistle as a high-frequency excitation actuator: a, b) Schlieren photographs of two phases of oscillation of the Hartmann whistle (supply jet on left, resonance tube on right) and c) spectrum of signal from microphone in the nearfield. Supply pressure = 20 psig, $\Delta x/D$ = 1, D = 0.254 cm, d = 1.5113 cm, f = 4.32 kHz, and d/D = 6:1 (D, diameter; d, depth).

single and multiple PRTB of various lengths, shapes, and diameters. The configurations tested are described in Table 1.

Experimental Details

The resonance tubes examined in this paper mainly consist of cylindrical tubes of various diameters and depths. A few tapered and stepped resonance tubes were also examined. More complex configurations including several versions of the PRTBs were also studied. For the single resonance tubes the microphone was located at $y = 0$, $x = 0.625$ in. (1.5875 cm) and $z = 0.5625$ in. (1.4288 cm), where x is along the length of the resonance tube, y is the transverse dimension, and z is the vertical dimension. The origin is at the center of the entrance to the resonance tube. For the resonator bank the microphone was located at $y = 0$, $x = -0.625$ in. (-1.5875 cm), and $z = 0.3750$ in. (0.9525 cm). Figure 3 shows the experimental setup at IIT. The microphone location is shown in Fig. 3a. The setup pictured consisted of a supply jet of $\frac{1}{4}$ in. (0.6350 cm) diam aimed at a resonance tube of $\frac{1}{2}$ in. (1.27 cm) depth, $\frac{1}{4}$ in. (0.6350 cm) diam. The distance between the supply jet and the resonance tubes could be varied in small increments. Drawings for various resonance tube shapes shown in Figs. 3b–3d include cylindrical, tapered (conical), and stepped.

One of the problems with the single resonance tube that we used was that the spillage of air occurred circumferentially all around the tube. In a practical application such a device would have to be embedded in a cavity or nozzle (for example), and pulsations are desired only on one side of the device. To facilitate such action, a shielded resonance tube was designed and tested. It was found that the shield did not affect the operation of this device or the sound-pressure levels (SPLs) produced by this device. The shielded powered resonance-tube idea was advanced a step further by building an integrated device that housed seven resonance tubes. Figure 4 shows the integrated Boeing/IIT powered resonance-tube actuator. Schematic, assembled, and exploded views are used to describe the apparatus. Figure 4a shows that all resonance tubes in the PRTB share the same plenum. A perforated plate is used to condition the incoming flow. The PRTB 1A actuator that is pictured in Fig. 4 consists of seven $\frac{1}{4}$-in. (0.6350-cm) tubes set at a spacing of $\frac{1}{2}$ in. (1.27 cm) (from center to center) or $\frac{1}{4}$ in. (0.6350 cm) from edge to edge. The actuator edge to nozzle spacing for supply nozzles 1 and 7 was also $\frac{1}{2}$ in. (1.27 cm). There are some important differences between the design of single resonance tubes and the PRTBs. First, PRTB 1A consists of seven convergent–divergent supply jet nozzles that are designed to operate shock free at $M = 2$. Second, a thin needle was inserted along the axis of each jet nozzle. This improvement was originally proposed by Brocher et al.[7] to prevent operation problems at occur at supersonic Mach numbers. (At supersonic supply-jet Mach numbers the functioning of the tube was hindered by the presence of a shock near the mouth of the resonance tube.) The cylindrical needle works by reducing the total head of

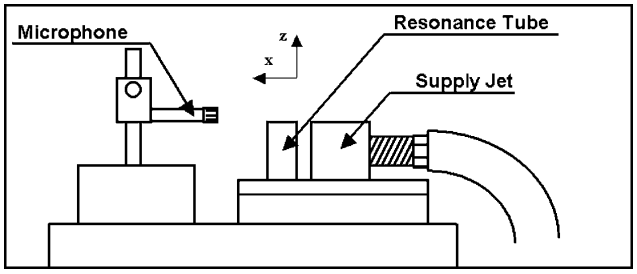

a)

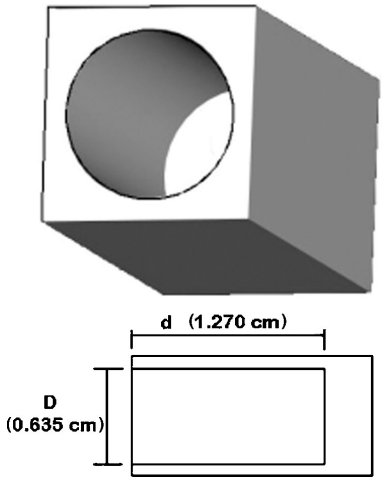

b)

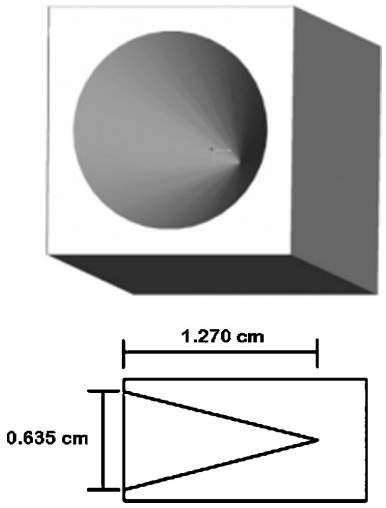

c)

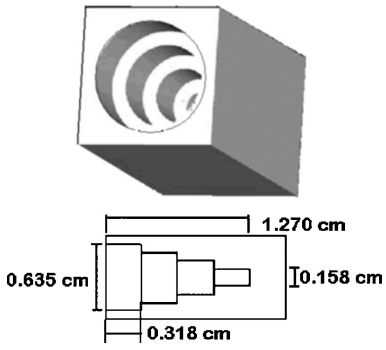

d)

Fig. 3 Single resonance-tube actuator and geometries: a) schematic of single resonance-tube actuator (supply jet on right, resonance tube on left), b) cylindrical resonator with diameter *D* and depth *d*, c) tapered (conical) resonator, and d) stepped resonator.

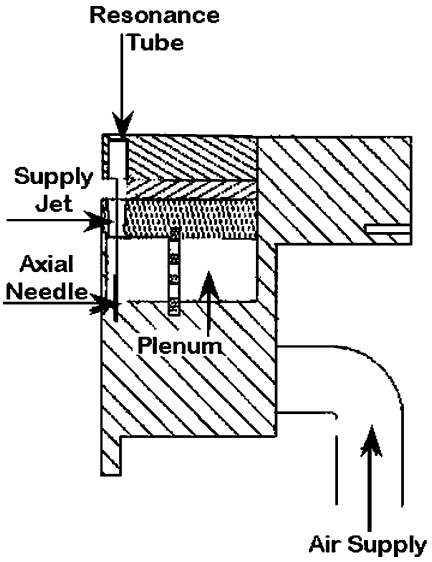

a)

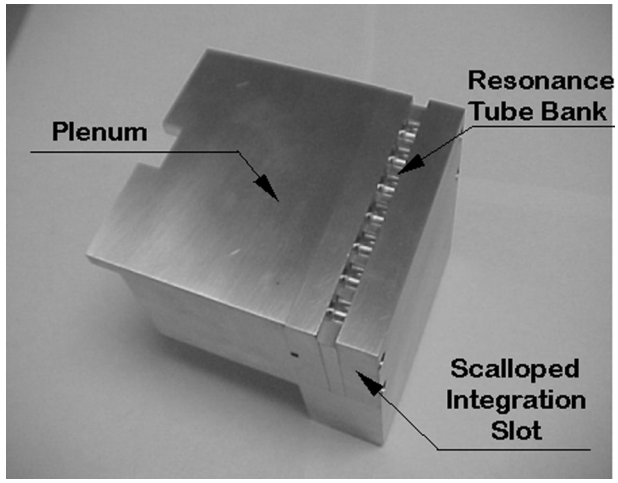

b)

Fig. 4 Boeing/IIT powered resonance-tube bank (PRTB IA): a) schematic diagram of PRTB and b) photograph of assembled PRTB.

the jet coming out of the nozzle around the axis. Thus, the total head in this region will be lower than that coming out of the resonance tube during the expansion (or tube evacuation) phase. The flow from the resonance will be able to push the supply jet back farther during the expansion phase. This will result in a more complete evacuation of the resonance tube, and the supply jet will then be able to penetrate the resonance tube fully during the compression phase. Note that the enhancements are not always necessary. Both the single-nozzle actuators and the PRTB IB, C used convergent nozzles without a needle. However, all PRTBs had a scalloped plate that guided the supply jets to the resonance tubes. The single-nozzle actuators used a supply nozzle with a slight chamfer at the exit. Other variations of the PRTB IA actuator bank were also built and tested. These actuators (PRTB I B, C) were switchable between 9 and 5, $\frac{1}{8}$-in. (0.3175-cm) resonance tubes. The nine nozzles in the nine-nozzle PRTB 1B actuator were spaced 0.4 in. (1.016 cm) apart when measured from center to center. The actuator-edge to nozzle-center spacing for supply nozzles 1 and 9 was also 0.4 in. (1.016 cm), whereas for the five-nozzle PRTB IC configuration the jet spacing was 0.8 in. (2.032 cm) when measured center to center. The actuator-edge to nozzle-center spacing was 0.4 in. (1.016 cm) for supply nozzles 1 and 5. The Gen-II actuator was similar in design to the Gen-IA actuator with the following improvements. The Gen-II actuator could be operated with either 7 or 15 resonance tubes. In addition, a bleed provision allowed for controlled variation of

mass injected into the flow without changing the supply pressure to the actuator. The variables in our experiment included the nozzle pressure ratio, the spacing between the supply jet, and the powered resonance tubes. A limited study was conducted on the effect of resonance-tube shape, diameter, and tube depth. For all resonance tubes studied, the diameter of the supply jet was the same as that of the inlet of the resonance tube.

The precision of the omnidirectional B & K microphones used in the present study is 0.5 dB. Consequently, the zeroth order estimate of the error is SPL = SPL $\pm$ 1 dB for the frequency range from 0–10 kHz. The resolution of the frequency spectra provided a zeroth-order estimate of 4 Hz. The error in setting the supply pressure was 0.2 psi. A statistical analysis of the data included a standard deviation, and the values quoted for the repeatability tests are based on the 95% confidence interval of twice the standard deviation. From the repeatability tests the frequency error was less than 20 Hz (0.4% at a resonance frequency of 5 kHz) for the high-amplitude steady cases. For some cases this error rose to 60 Hz (1.2% at 5 kHz). The error in measuring the amplitude of resonance was about 2 dB. The total errors were 2.23 dB for the SPL and 60.14 Hz for the frequency. For the measurements reported in this paper, sampling was at 50 kHz, and the antialias filter was set at 25 kHz.

Results and Discussion

Single-Resonance-Tube Actuator Characteristics

Table 1 provides a summary of powered resonance-tube configurations considered in the present work. This includes single-powered resonance tubes of various diameters, lengths, and shapes as well as several versions of the Boeing/IIT PRTB. Our goal was to document the frequency and amplitude of fluctuations produced by various configurations. Detailed data will now be presented for various configurations in the following format. Frequency and SPL maps will be documented for various operating pressures and supply jet to resonance-tube spacings. Each set of maps will be followed by a typical spectrum for the case under consideration. The frequency and SPL maps are for the primary frequency in the spectrum. Harmonics are present in many cases but are not documented herein except in the sample spectra. Many of the frequency and amplitude maps exhibit "null" regions, where the resonance tube does not produce oscillations, and these regions appear in white color in the plots. This result agrees with Hartmann's observation that in order to obtain high-amplitude oscillations the inlet of the resonance tube should be located in the compression region of the supply-jet's shock cell-system. Thus, not all spacings produce sharp tones. Figures 5 and 6 show such data for a deep and shallow resonance tube, respectively. Although the documentation of frequency is quite straightforward,

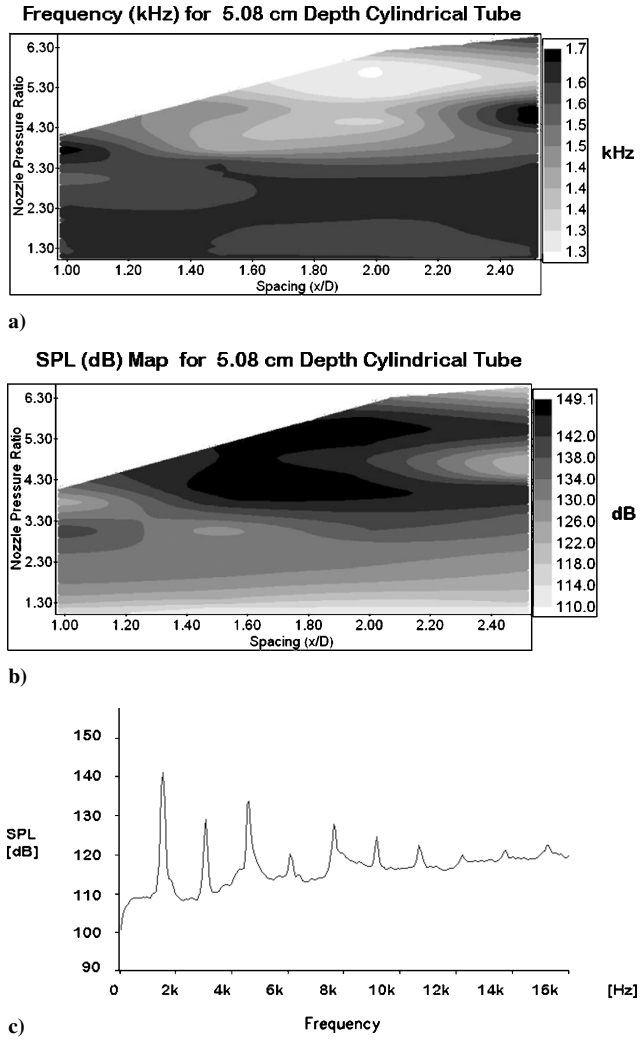

Fig. 5 Performance characteristics for single cylindrical powered resonance-tube actuators. Resonance-tube depth/diameter ratio *d*/*D* = 8. Resonance tube and supply-jet diameter = 0.635 cm. a) Actuator frequency. b) Actuator amplitude for various nozzle pressure ratios and jet-resonance-tube spacings. c) Microphone spectrum at NPR = 3.079; spacing between supply jet and resonance tube *x*/*D* = 1.

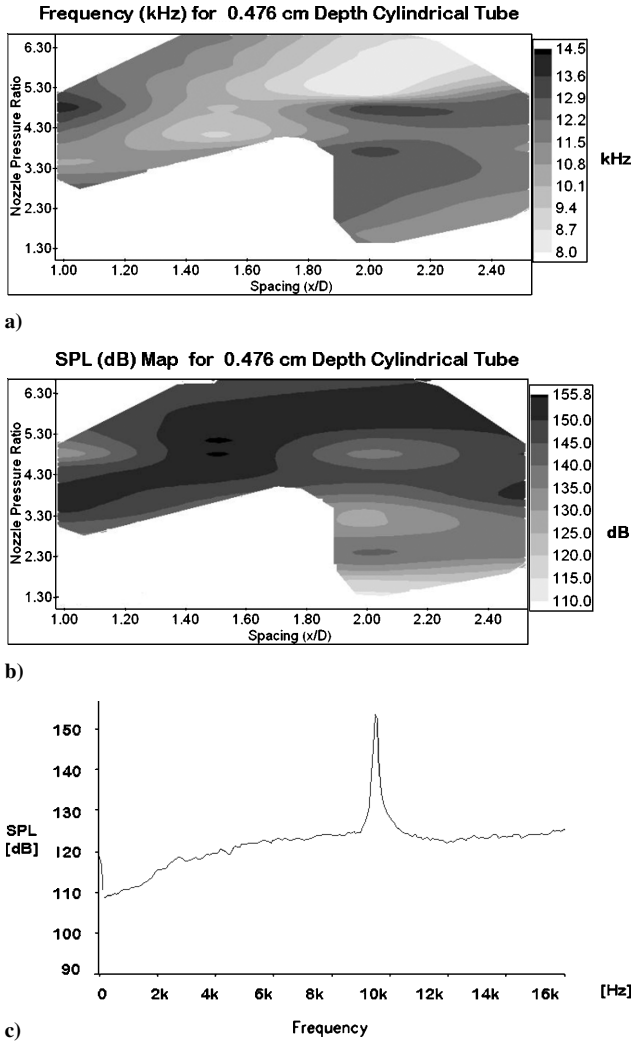

Fig. 6 Performance characteristics for single cylindrical powered resonance-tube actuators. Resonance-tube depth/diameter ratio *d*/*D* = 0.75. Resonance tube and supply-jet diameter = 0.635 cm. a) Actuator frequency. b) Actuator amplitude for various nozzle pressure ratios and jet-resonance-tube spacings. c) Microphone spectrum at NPR = 4.460; spacing between supply jet and resonance tube *x*/*D* = 1.5.

Table 2 Actuator amplitude metrics {cylindrical resonance-tube spacing [x = 0.375 in. (0.953 cm), x/D = 1.5]}

Pressure, psig (NPR)	Frequency, Hz	SPL, dB	Prms, Pa	Power, W	Energy density
45 (4.114)	4928	135	112.46	0.1747	0.1008
50 (4.460)	5120	152	796.21	8.7558	5.0082
55 (4.806)	5184	154	1002.37	13.8770	7.9160
60 (5.152)	5312	156	1261.91	21.9936	12.481

no single standard metric exists for the documentation of amplitude. In the absence of such a standard, we report the amplitude as sound-pressure level (SPL, dB), p'_{rms}, sound power W, and acoustic energy density E.

Table 2 provides representative data on the performance of powered resonance-tube actuators. The amplitude of actuation is characterized using metrics from linear acoustic theory such as acoustic power W and acoustic energy density E. These quantities are derived from the SPL as follows: $\text{SPL} = 20\ \text{Log}_{10}(p_{\text{rms}}/p_{\text{ref}})$, where $p_{\text{ref}} = 20\ \mu\text{Pa}$. The acoustic power $W = (p^2_{\text{rms}}/\rho_0 c)4\pi R^2$, where R is the distance from the microphone to the resonance tube, ρ_0 is the density of air (1.21 Kg/m^3), and c is the ambient speed of sound (343 m/s). The acoustic energy $E = p^2_{\text{rms}}/\rho_0 c^2(1 + \frac{1}{2}k^2 r^2)$, where r is the distance from the source, $k = \omega/c =$ wave number, and $\omega = 2\pi f$, where f is the frequency. The metrics just described are subject to several assumptions (including spherical radiation of sound into open space). The usefulness of the sound-power metric is that it eliminates the microphone location as a parameter. (SPL depends on the microphone location, but the sound-power level is a characteristic of the source that is independent of microphone location.) The energy density E metric includes the effect of frequency and provides the average acoustic energy present in a unit volume of the medium. An illustration of the usefulness of the amplitude metrics is provided in the following example. Consider three actuators operating at different frequencies and producing 154 dB. Although this corresponds to 13.87 W for all actuators, the energy density for each case is different because the actuators operate at different frequencies. The acoustic efficiency of a typical PRT device can be calculated by taking the ratio of the output power to the input power. Input power is given by the product of pressure and volume flow rate. The acoustic efficiency of the PRT device ranges from 3 to 9% depending on operating conditions. Although the numbers might seem small this is quite large for a fluid-powered device because sound production by a jet is a small fraction of the kinetic energy of the jet.

For the frequency one can obtain approximate relationships for the eigen-frequencies using linear acoustic theory ($f = c/4L$); the measured results do not always agree with the predictions. For example, a resonance-tube length variation from 3/16 in. (0.4763 cm) to 2 in. (5.08 cm) [for the $\frac{1}{4}$-in. (0.635-cm)-diam resonance tube and $\frac{1}{4}$-in. (0.635-cm)-diam supply jet, d/D variation from 0.75 to 8] produced a measured frequency change from about 10 to 1.6 kHz. The corresponding quarter-wavelength frequencies obtained from $f = c/4L$ were 17.6 kHz [3/16 in. (0.476 cm), $d/D = 0.75$] and 1.65 kHz [2 in. (5.08 cm), $d/D = 8$]. Thus for long tubes the measured and calculated values appear to agree. However, there is considerable departure for short tubes. No end correction was used for our calculations. It is believed that the use of an end correction will significantly improve the predictions for shallow resonance tubes. In this context it should be noted that there are other phenomena, such as screech tones, where the acoustic amplitudes are very large and frequencies based on shock-cell spacings obtained from linear theory are quite accurate (with an adjustable constant). A recent paper by Raman et al.[22] provides a suitable correction using the Kerschen method that accounts for the interaction of the resonance tube with the integration slot and the compliance of the mass of fluid in the integration slot.

A few spot checks with longer tubes revealed that an actuator frequency of 500 Hz could be obtained with a 6-in. (15.24 cm; $d/D = 24$)-long resonance tube. In the present work the tube depth was changed by building several tubes ranging in depth from 3/16 to 6 in. (0.47625 to 15.24 cm). A slightly different approach was used in the experiments done at Boeing[16] and in the more recent work

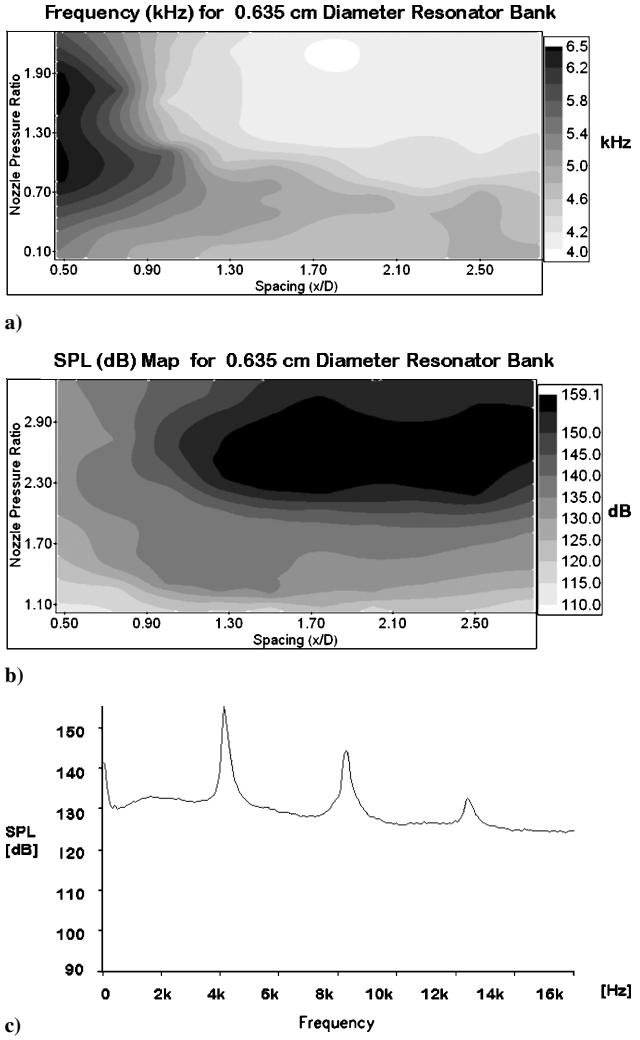

Fig. 7 Performance characteristics for the Boeing/IIT PRTB IA integrated actuator with seven resonance tubes. Resonance-tube depth/diameter ratio d/D = 2. Resonance tube and supply-jet diameter-0.635 cm. a) Actuator frequency. b) Actuator amplitude for various nozzle pressure ratios and jet-resonance-tube spacings. c) Microphone spectrum at NPR = 2.287; spacing between supply jet and resonance tube x/D = 1.5.

of Raman et al.,[22] where a computer-controlled piston and cylinder assembly was used to change the depth of the tube.

We now proceed to compare the performance of tapered (conical) and stepped tubes all having a depth of 0.5 in. (1.27 cm) and a tube opening diameter of 0.25 in. (0.635 cm; see Figs. 3c, and 3d). The shaping of the tube appears to change its effective length. It was very clear that the tube shape had a great effect on the frequency of resonance. Both the stepped and the tapered tubes resonated in a frequency range from about 7–11 kHz, whereas the cylindrical tube resonated in the range 4.352–6.080 kHz. Surprisingly the peak amplitudes produced by the three tubes were the same (156 dB).

In an effort to lower the mass flow though the actuator, we examined various diameters. For all cases the supply-jet diameter was always the same as that of the resonance tube. Data were acquired for tubes ranging from 0.25 to 0.0625 in. (0.635 to 0.1588 cm). For

the 0.25-in. (0.635-cm)-diam tube the oscillations were strong only above 30 psig. In contrast, for the 0.125- and 0.0625-in. (0.3175- and 0.1588-cm)-diam tubes the onset of oscillations occurred at lower pressures {5 psig [1.346 nozzle pressure ratio (NPR)]}.

Resonance-Tube Actuator Banks

A more complex version of this device known as the powered resonance-tube bank (PRTB) that easily integrates into practical applications was developed and demonstrated.[17] Two generations of PRTBs were developed. This included three versions of the generation I device (IA-C) and a version of the generation II device. Version IA consisted of a bank of seven $\frac{1}{4}$-in. (0.635-cm)-diam jets aimed seven resonance tubes of $\frac{1}{2}$-in. (1.270-cm) depth having the same diameter. For the range of pressures tested, the mass flow varied from 0.0611 kg/s at 14.2 psig (1.983 NPR) to about 0.1857 kg/s at 71.3 psig (5.934 NPR). The IB and IC PRTBs, designed with the idea of reducing the mass flow without loss of actuation effectiveness, had nine and five $\frac{1}{8}$-in. (0.3175-cm) jets, respectively. The mass flow through the nine and five tube PRTBs (IB, C) were lower by 51 and 67% at 15 psig (2.038 NPR) and lower by 42 and 65% at 30 psig (3.076 NPR), respectively.

Data from the PRTB actuators are given in Figs. 7 and 8. The 0.25-in. (0.635-cm) PRTB (1A) produced a SPL of 159 dB at 20 psig (2.384 NPR). In contrast the 0.125-in. (0.3175-cm) PRTB with five tubes (IC) produced a peak level of 149 dB at 20 psig (2.384 NPR). It is seen from the operating maps for PRTB IA,C actuators that for resonance tubes of constant depth vast regions of relatively high amplitude exist at approximately constant frequencies.

Application of PRTs for Cavity and Impingement Noise Suppression

We will now provide two concrete illustrations of applications where the PRTB actuator was used successfully.

In the first application the Gen-IA device was tested in a DERA (United Kingdom) weapons bay cavity (length/depth = 5, length/width = 5, width = 4 in. or 10.16 cm) tested at Aircraft Research Association (ARA; United Kingdom) transonic wind tunnel (see Refs. 18 and 19 for a detailed account). The cavity had bay doors that were fixed at 90 deg. Cavity tone suppression tests were run at freestream Mach numbers ranging from $M = 0.4$ to 1.35. Figure 9 shows photographs of the cavity model in the ARA transonic wind tunnel. The Gen-IA actuator was installed upstream of the cavity (Fig. 9c). The Gen-IA device was operated with a $\frac{1}{4}$-in. (0.635-cm) spacer at an NPR range from about 1.9 to 7.0. The corresponding actuator plenum pressure and mass flow ranged from 14.2 to 71 psig (1.983 to 5.913 NPR) and 0.0611 to 0.1857 kg/s, respectively. The

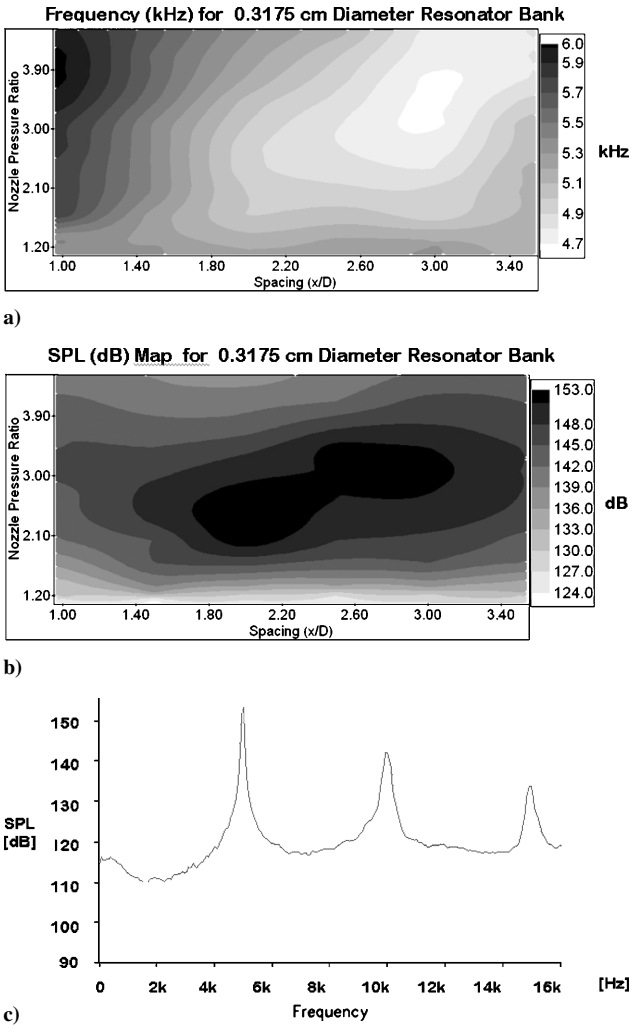

Fig. 8 Performance characteristics for the Boeing/IIT PRTB IB integrated actuator with nine resonance tubes. Resonance-tube depth/diameter ratio $d/D = 4$. Resonance tube and supply-jet diameter-0.318 cm. a) Actuator frequency. b) Actuator amplitude for various nozzle pressure ratios and jet-resonance-tube spacings. c) Microphone spectrum at NPR = 2.0381; spacing between supply jet and resonance tube $x/D = 2$.

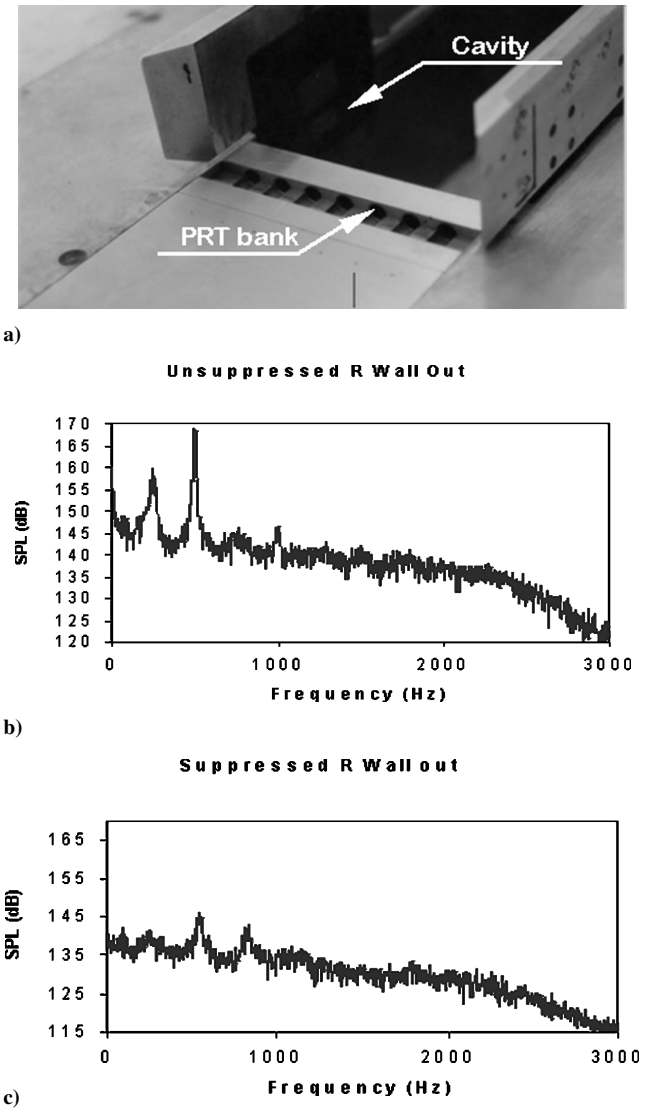

Fig. 9 Successful implementation of the Boeing/IIT PRTB IA in the DERA cavity at the ARA transonic wind tunnel[18]: a) photograph of the model in the transonic tunnel (note the installation of the PRTB upstream of the cavity) and d, e) unsuppressed and suppressed cavity noise spectra at wind tunnel $M = 1.19$.

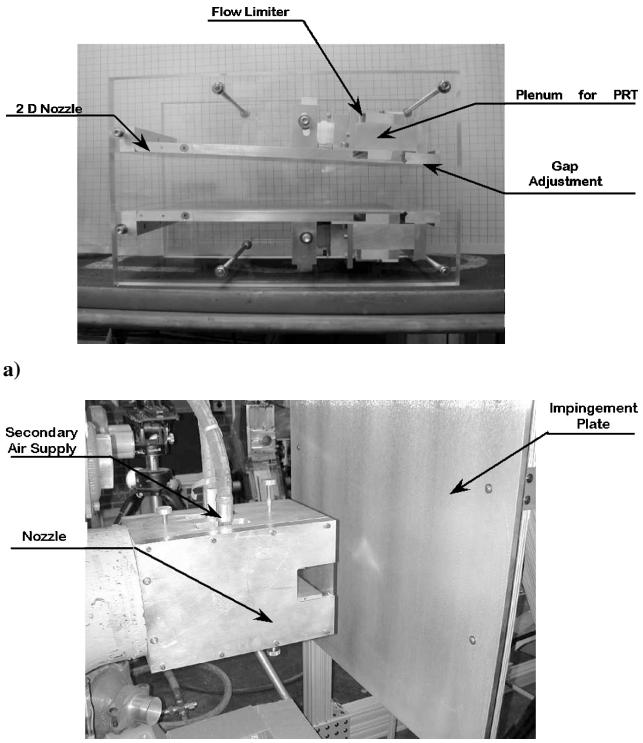

Fig. 10 Photographs of two-dimensional nozzle with integrated actuator and jet-impingement apparatus: a) view of nozzle details and b) impinging jet setup.

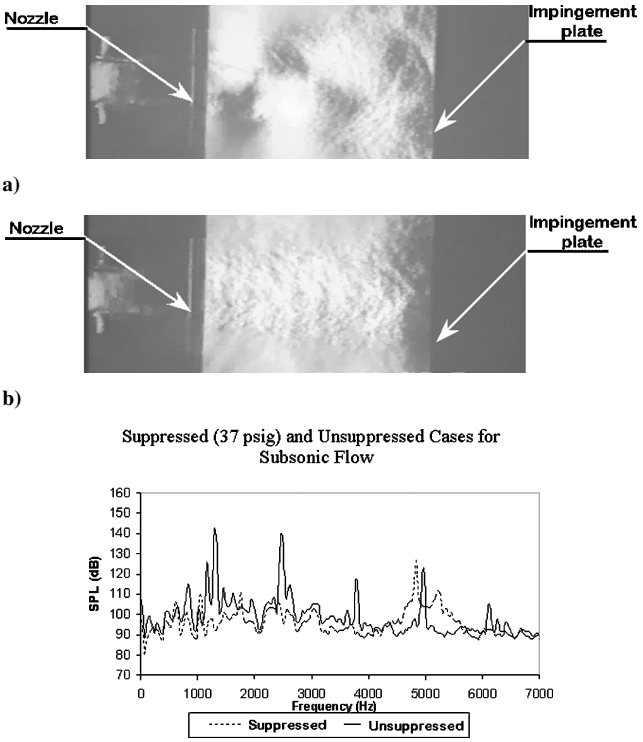

Fig. 11 Impingement noise suppression using powered resonance-tube actuators: a, b) Schlieren photographs for unsuppressed and suppressed cases and c) spectra for unsuppressed and suppressed cases.

cavity tones (250 and 500 Hz) were suppressed by 25 dB at the rear wall and by 28 dB on the floor of the cavity at x = 3 in. (7.62 cm) (x/cavity length = 0.15) from the upstream end of the cavity. Spectra are shown for the rear-wall location in Figs. 9d and 9e for the unsuppressed and actuator suppressed cases. The suppression occurred at a cost of 0.1417 kg/s mass flow through the actuators. The excitation signal itself was at 5 kHz (over an order of magnitude higher than the cavity tone) and is not within the scale of the x axis because our focus here is on the cavity tones. Multiple cavity tones in the range from 250–1000 Hz were simultaneously suppressed using high-frequency excitation around 5 kHz.

A second test was designed with the objective of evaluating the effectiveness of the Gen–II high-frequency actuator in suppressing jet-impingement tones. Experiments were conducted in the Boeing "flute room" at St. Louis. The flute room is a high-speed flow facility capable of high mass-flow rates. A two-dimensional jet nozzle was installed at the end of a settling chamber. The flow from the nozzle impinged on a vertically mounted ground plate. Two Boeing-II PRT actuators were integrated within and on either side of the long dimension of the rectangular nozzle (variable exit dimensions). The nozzle and impingement plate apparatus are shown in Fig. 10. The assembled view of the nozzle with the Gen-II actuator appears in Fig. 10a. The Plexiglas® side wall was only used for display purposes. In the actual test two 1-in.-thick Al plates were used (see Fig. 10b). Figure 10b also shows the impinging jet setup and the actuator pressure supply lines at the top of the nozzle. The slot seen on the top inside wall of the actuator represents the gap between the supply jet and the resonance tube. The Lexan windows were inserted for flow visualization.

The effectiveness of a single actuator bank located on the top wall of the nozzle is shown in Fig. 11. Phase-conditioned schlieren photographs show that large-scale antisymmetic oscillations produced by the $M = 0.98$ impinging jet are completely eliminated when the high-frequency actuation is turned on. In Fig. 11c the thick line represents the unsuppressed case and the dashed line the suppressed case. The primary impingement tone was at about 1.3 kHz and the actuation frequency range from 5–5.3 kHz. The corresponding ratio of excitation frequency/frequency of the impingement tone varied from 3.85–4.07. Increasing actuator pressures from 6–37 psig resulted in complete destruction of the impingement tone. Similar data were also obtained for a $M = 1.09$ jet (not shown for brevity). For the subsonic impinging jet it was observed that suppression begins at a mass-flow rate of 0.01 kg/s and is complete at 0.07 kg/s (2.02% of the main jet's mass flow). In contrast, for the supersonic jet case suppression begins at 0.065 kg/s and is complete at 0.13 kg/s (3.6% of the main jet's mass flow). Further efforts should focus on reducing the mass-flow requirements.

Conclusions

The present paper addressed both high-frequency actuator technology development and the demonstration of the effectiveness of actuators that could be easily integrated into practical applications. The parameters that influenced the operation of a single subelement that could be integrated into a more complex device were first examined. The parameters included the effect of tube length, diameter, shape, integration slot spacing, and supply pressure. The output of the actuator was characterized by an oscillation frequency and amplitude. Metrics used to characterize the amplitude included sound pressure level p'_{rms}, acoustic power, and acoustic energy density.

Following our studies on single PRTs, two generations (Gen-I and Gen-II) of linear arrays of powered resonance-tube banks (PRTBs) were developed. Gen-I included three versions of PRTBs. The first (IA) consisted of a bank of seven $\frac{1}{4}$-in. (0.635-cm)-diam jets that injected a mass flow of 0.0612 kg/s at 15 psig (2.038 NPR) and 0.0924 kg/s at 30 psig (3.076 NPR). The IB and IC PRTBs, designed with the idea of reducing the mass flow without loss of actuation effectiveness, had nine and five $\frac{1}{8}$-in. (0.3175-cm) jets, respectively. The mass flow through the nine and five tube PRTBs (IB,C) were lower by 51 and 67% at 15 psig (2.038 NPR) and lower by 42 and 65% at 30 psig (3.076 NPR), respectively. A Gen-II PRTB that used either 7 or 15 $\frac{1}{4}$-in. resonance tubes and that had mechanisms for regulating the mass flow was also developed. The mass flow with no air bleed for the seven-tube Gen-II PRTB was the same as that for Gen-I but could be reduced using the bleed provision.

Two demonstration experiments were designed to test the effectiveness of the PRTBs. Both experiments were situations that involved the production of flow-induced resonance (cavity tones and impinging jets). The first demonstration evaluated the Gen-I PRTB in a transonic wind tunnel using a length to depth ratio of and 5 rectangular cavity at $M = 1.19$. Tonal suppression levels of over 25 dB were recorded. In the second experiment the Gen-II PRTB was tested in a jet-impingement apparatus. The jet was operated at $M = 0.98$ and impinged on a ground plane. Tonal suppression of over 30 dB was recorded.

Our results suggest that the outlook for high-frequency actuators in shear flow-control applications is very promising. The conventional actuators are fragile, have higher power and maintenance requirements, and are thus relegated to laboratory demonstrations. In contrast, the optimized PRTB can reach higher technology readiness levels for application on future aircraft's flow and noise control systems.

Acknowledgments

Illinois Institute of Technology was a part of the Boeing team funded by the Defense Advanced Research Projects Agency. William W. Bower served as program manager for the Boeing team. The NASA Space Grant supported Andrew Mills's role as undergraduate research participant. The authors also thank Craig Johnson and Ron Mashek for their expertise in machining the Illinois Institute of Technology/Boeing IB,C device.

References

[1]Hartmann, J., and Troll, B., "On a New Method for the Generation of Sound Waves," *Physical Review*, Vol. 20, 1922, pp. 719–727.

[2]Hartmann, J., "On the Production of Acoustic Waves by Means of an Air-Jet of a Velocity Exceeding That of Sound," *Philosophical Magazine and Journal of Science XI*, 1931, p. 926.

[3]Sprenger, H., "Ueber Themische Effekete in Resonszrohren," Mitt, Inst. Aerodynamik, E.T.H., Vol. 21, 1954, p. 18.

[4]Iwamoto, J., and Deckker, B. E. L., "A Study of the Hartmann-Sprenger Tube Using the Hydraulic Analogy," *Experiments in Fluids*, Vol. 3, 1985, pp. 245–252.

[5]Iwamoto, J., "Experimental Study in a Rectangular Jet-Driven Tube," *Journal of Fluids Engineering*, Vol. 112, No. 1, 1990, pp. 23–27.

[6]Rakowsky, E. L., Corrado, A. P., and Marchese, V. P., "Fluidic Explosive Initiator," *Fluidics Quarterly*, Vol. 6, 1974, pp. 13–32.

[7]Brocher, E., Maresca, C., and Bournay, M. H., "Fluid Dynamics of the Resonance Tube," *Journal of Fluid Mechanics*, Vol. 43, pt. 2, 1970, pp. 369–384.

[8]Brocher, E., and Duport, E., "Resonance Tubes in a Subsonic Flowfield," *AIAA Journal*, Vol. 26, No. 3, 1988, pp. 548–551.

[9]Thompson, M. C., Hourigan, K., Welsh, M. C., and Brocher, E., Acoustic Sources in a Tripped Flow Past a Resonator Tube," *AIAA Journal*, Vol. 30, No. 6, 1992, pp. 1484–1491.

[10]Brocher, E., and Maresca, C., "Comments on Experimental Investigation of a cylindrical resonator," *AIAA Journal*, Vol. 13, No. 8, 1975, 1127.

[11]Brocher, E., "Heating Rate of Driven Gas in a Hartmann-Sprenger Tube," *AIAA Journal*, Vol. 13, No. 10, 1975, pp. 1265, 1266.

[12]Kawahashi, M., Bobone, R., and Brocher, E., "Oscillation Modes in Single-Step Hartmann-Sprenger Tubes," *Journal of the Acoustical Society of America*, Vol. 75., No. 3, 1984, pp. 780–784.

[13]Kawahashi, M., Brocher, E., and Collini, P., "Visualization of Vortex-Shedding from Wedge Coupling with Resonator," *Journal of Flow Visualization*, Vol. 7, No. 26, 1987, pp. 243–246.

[14]Wiltse, J. M., and Glezer, A., "Manipulation of Free Shear Flows Using Piezoelectric Actuators," *Journal of Fluid Mechanics*, Vol. 249, 1993, pp. 261–285.

[15]Wiltse, J. M., and Glezer, A., "Direct Excitation of Small-Scale Motions in Free Shear Flows," *Physics of Fluids*, Vol. 10, No. 8, 1998, pp. 2026–2036.

[16]Raman, G., Kibens, V., Cain, A., and Lepicovsky, J., "Advanced Actuator Concepts for Active Aeroacoustic Control," AIAA Paper 2000-1930, June 2000.

[17]Kibens, V., and Raman, G., "High Frequency Excitation Apparatus and Method for Reducing Jet and Cavity Noise," U.S. Patent No. 6,375,118 B1, 23 April 2002.

[18]Stanek, M., Raman, G., Kibens, V., Ross, J., Peto, J., and Odedra, J., Cavity Tone Suppression Using High Frequency Excitation," AIAA Paper 2000-1905, 2000.

[19]Stanek, M., Raman, G., Kibens, V., Ross, J., Peto, J., and Odedra, J., "Suppression of Cavity Resonance Using High Frequency Forcing—The Characteristic Signature of Effective Devices," AIAA Paper 2001-2128, 2001.

[20]Cain, A. B., Rogers, M. M., Kibens, V., and Raman, G., "Simulations of High-Frequency Excitation of a Plane Wake," AIAA Paper 2001-0514, 2001.

[21]Kastner, J., and Samimy, M., "Development and Characterization of Hartmann Tube Based Fluidic Actuators for High Speed Flow Control," *AIAA Journal*, Vol. 40, No. 10, 2002, pp. 1926–1934; also AIAA Paper 2002-0128, 2002.

[22]Raman, G., Khanafseh, S., Cain, A., and Kerschen, E., "Development of High Bandwidth Powered Resonance Tube Actuators with Feedback Control," *Journal of Sound and Vibration*, Vol. 269, Jan. 2004, pp. 1031–1062.